Available online at www.sciencedirect.com
SCIENCE DIRECT®
Journal of Non-Crystalline Solids 352 (2006) 78–83
JOURNAL OF NON-CRYSTALLINE SOLIDS
www.elsevier.com/locate/jnoncrysol

Boron content dependance of magnetoimpedance in $Fe_{91-x}Zr_5B_xNb_4$ alloys

K. Zhang [a], Z. Lv [b], B. Yao [a,c,*], D. Wang [a]

[a] Department of Physics, Jilin University, No. 2519, Jiefang Road, Changchun, Jilin 130023, PR China
[b] Center for Condensed-Matter Science and Technology, Harbin University of Technology, Harbin 150001, PR China
[c] Key Laboratory of Excited State Process, Chinese Academy of Sciences, Changchun Institute of Optics, Fine Mechanics and Physics, Chinese Academy of Sciences, Changchun 130022, PR China

Received 8 April 2005; received in revised form 20 October 2005
Available online 7 December 2005

Abstract

A systematic investigation of the influence of B content on the magnetoimpedance (MI) effect in melt-spun $Fe_{91-x}Zr_5B_xNb_4$ (FZBN, $0 \leqslant x \leqslant 30$) ribbons has been performed within a frequency range, $f \sim 310$–1110 kHz and under a varying dc magnetic field (H_{dc}) up to 70 Oe. The MI effect is not observed in the sample with $x \leqslant 5$ but within the range $8 \leqslant x \leqslant 30$. A distinct MI effect has been observed with a maximum change of 180% at around 1.1 MHz in the sample with $x = 20$, coincident with a saturation magnetic field of 66 Oe and a field sensitivity of about 7%/Oe. Magnetic measurements reveal that the MI effect and B content dependence of the effect are closely related to coercivity of the FZBN alloy series, except for the sample with 20 at.%. The drastic MI ratio observed in the sample with $x = 20$ is ascribed to its special microstructure. The mechanism of the MI effect in FZBN alloys and of the significant MI value appearing at a B content of $x = 20$ is discussed in this paper.

PACS: 61.43.Dq; 71.23.Cq; 75.47.Np; 75.50.Ss

Keywords: Amorphous metals; Metallic glasses; Alloys; Glass formation; Glass transition; Magnetic properties

1. Introduction

The magnetoimpedance (MI) effect is the large variation of impedance in soft magnetic materials induced by a small dc magnetic field in the presence of a relatively high frequency ac field. In general, it is characterized by a rapid decrease of impedance with increasing applied magnetic field. It is generally attributed to the decrease of transverse or circumferential ac permeability as longitudinal the dc magnetic field rises, resulting in an increasing skin depth, and decline in impedance [1]. Since the MI effect was observed first in 1992 by Mohri et al. in Co-based amorphous wire [2], it has attracted considerable attention for its important potential applications in high sensitivity micromagnetic sensors and magnetic recording heads. It has also been investigated in a variety of Fe and Co-based amorphous ribbons [3], thin films [4], multilayer films with sandwiched structures [5] and wires [6]. Many of previous works have demonstrated that the MI effect is related to such magnetic properties of materials, as coercivity, saturation magnetostriction, and transverse (for ribbon and thin film) permeability or circumferential (for wire) permeability.

The MI effect in Co-based amorphous alloys has been extensively studied in the past. Whereas its investigation in Fe-based amorphous alloys is yet to be pursued. It is concluded from the literatures on Co-based amorphous alloys that metallic glass with near zero magnetostriction

* Corresponding author. Address: Department of Physics, Jilin University, No. 2519, Jiefang Road, Changchun, Jilin 130023, PR China.
E-mail address: binyao@mail.jlu.edu.cn (B. Yao).

0022-3093/$ - see front matter © 2005 Elsevier B.V. All rights reserved.
doi:10.1016/j.jnoncrysol.2005.10.023

show large MI ratios [7]. For example, a MI ratio as high as 360% was observed in Co-based amorphous wire or ribbon with a zero magnetostriction constant. However, a distinct MI effect has not been achieved in any as-spun Fe-based amorphous alloys due to their large positive magnetostriction up to now, with the exception of annealed Fe–Cu–Nb–Si–B and Fe–Zr–B–Cu amorphous alloys [8,9]. The large MI ratio obtained in these annealed Fe-based amorphous alloys is ascribed to the decline in magnetostriction and an increase in transverse or circumferential permeability [1].

It is well known that soft magnetic properties, which are closely related to the composition and internal configuration of amorphous alloys, are essential for a large MI effect. According to our previous research results, we conclude that $Fe_{91-x}Zr_5B_xNb_4$ (FZBN) alloys possess good soft magnetic properties that change with their composition. The purpose of this work is to investigate the composition dependence of both the MI effect and the magnetic properties of FZBN alloys. We will also explore the relationship between the MI effect and the magnetic properties in Fe-based amorphous alloys.

2. Experimental procedures

Polycrystalline ingots of nominal composition $Fe_{91-x}Zr_5B_xNb_4$ (FZBN) ($0 \leqslant x \leqslant 30$ at.%) were prepared in an induction melting furnace under Ar atmosphere. The ingots of the alloys were remelted 10 times to ensure the homogeneous composition in the samples. Amorphous ribbons were obtained using single roller melt-spinning equipment with a copper wheel rotating at a surface velocity of 30 m/s. Each sample is 20–25 μm in thickness and 2 mm in width.

The amorphous and crystalline structures were identified by X-ray diffractometry with Cu K_α radiation (XRD) and transmission electron microscopy (TEM). Measurements of glass transition temperature (T_g), crystallization temperature (T_x) and Curie temperature (T_c) were performed by differential scanning calorimeter (DSC) at a heating rate of 20 °C/min in a flowing argon atmosphere. In order to diminish the effect of the stress caused in rapid cooling process on Curie temperature, the value measured in the second run is taken as T_c. Magnetic properties of samples were measured by using vibrating sample magnetometer (VSM).

Table 1
Uncertainties of impedance $|Z|$, coercivity H_c and Curie temperature T_c of FZBN alloy with various B content

Uncertainties for data in Fig. 1											
H (Oe)	0	3.3	6.6	9.9	13.2	19.8	26.4	33	46.2	52.8	66
$\|Z\|(\Omega)_{[x=0]}$	0.3628		0.3631			0.3635			0.3639		0.3629
$\pm\Delta\|Z\|(\Omega)_{[x=0]}$	0.0036		0.0036			0.0036			0.0036		0.0036
$\|Z\|(\Omega)_{[x=8]}$	0.4084	0.3893	0.3806	0.3701	0.3644	0.3554	0.3483	0.3437		0.3325	0.3288
$\pm\Delta\|Z\|(\Omega)_{[x=8]}$	0.0041	0.0039	0.0038	0.0037	0.0036	0.0036	0.0035	0.0034		0.0033	0.0033
$\|Z\|(\Omega)_{[x=20]}$	0.4320	0.4093	0.3868	0.3600	0.3372	0.3037	0.2842	0.2728		0.2582	0.2537
$\pm\Delta\|Z\|(\Omega)_{[x=20]}$	0.0043	0.0041	0.0039	0.0036	0.0034	0.0030	0.0028	0.0027		0.0026	0.0025
Uncertainties for data in Fig. 3											
B content (at.%)	5	8	11	14	20	22.5	25	27	30		
H_c (Oe)	10.50	2.22	2.54	2.82	2.63	2.05	1.88	1.75	1.80		
$\pm\Delta H_c$ (Oe)	0.53	0.11	0.13	0.14	0.13	0.10	0.09	0.09	0.09		
T_c (°C)	11	44	61	79	130	168	185	211	247		
$\pm\Delta T_c$ (°C)	3	3	3	3	3	3	3	3	3		

Table 2
Uncertainties of crystallization temperature T_x, glass transition temperature T_g and saturated magnetization M_s of FZBN alloy with various B content

Uncertainties for data in Fig. 5										
B content (at.%)	5	8	11	14	17	20	22.5	25	27.5	30
T_x (°C)	569	573	582	558	562	568	625	632	636	649
$\pm\Delta T_x$ (°C)	2	2	2	2	2	2	2	2	2	2
T_g (°C)			562	545	547	546	582	589	590	608
$\pm\Delta T_g$ (°C)			2	2	2	2	2	2	2	2
Uncertainties for data in Fig. 6										
B content (at.%)	5	8	11	14	17	20	22.5	25	27.5	30
M_s (emu/g)$_{(RT)}$	37	59	69	84	86	93	104	106	104	113
$\pm\Delta M_s$ (emu/g)$_{(RT)}$	2	3	3	4	4	5	3	3	3	3
M_s (emu/g)$_{(78K)}$	120	126	128	132	129	130	135	140	146	146
$\pm\Delta M_s$ (emu/g)$_{(78K)}$	4	4	4	4	4	4	4	4	4	4

Table 3
Uncertainties of MI ratio $\Delta Z/Z(\%)$ of FZBN alloy with various B content

Uncertainties for data in Fig. 2											
B content (at.%)	0	5	8	11	14	17	20	22.5	25	27	30
MI $(\%)_{(310\text{kHz})}$	0.100	0.200	7.500	1.100	−0.200	0.010	4.200	9.900	4.300	1.300	2.000
$\pm\Delta$MI (%)	0.002	0.004	0.150	0.022	0.004	0.001	0.084	0.198	0.086	0.026	0.040
MI $(\%)_{(510\text{kHz})}$	−1.100	0.100	11.000	1.800	0.010	0.800	8.900	16.800	8.900	4.200	5.900
$\pm\Delta$MI (%)	0.022	0.002	0.220	0.036	0.001	0.016	0.178	0.336	0.178	0.084	0.118
MI $(\%)_{(810\text{kHz})}$	−0.900	0.700	19.000	7.900	2.900	2.500	50.000	27.600	16.800	10.700	15.800
$\pm\Delta$MI (%)	0.018	0.014	0.380	0.158	0.058	0.050	1.000	0.552	0.336	0.214	0.316
MI $(\%)_{(910\text{kHz})}$	−0.030	0.300	24.200	7.300	4.500	3.100	70.300	30.500	18.900	14.200	18.600
$\pm\Delta$MI (%)	0.001	0.006	0.484	0.146	0.090	0.062	1.406	0.610	0.378	0.284	0.372
MI $(\%)_{(1110\text{kHz})}$	−0.500	−0.800	20.900	9.600	8.500	4.700	183.800	35.800	23.000	17.800	18.100
$\pm\Delta$MI (%)	0.010	0.016	0.418	0.192	0.170	0.094	3.676	0.716	0.460	0.356	0.362

Solartron 1260 Impedance Analyzer was used for impedance measurements. A four-probe ac technique was used to measure the magnitude Z of the magnetoimpedance as function of the field H_{dc} applied along the ribbon length, i.e., parallel to the ac measuring current. The current amplitude used is $I = 3$ mA and frequency f is between 310 kHz and 1110 kHz. The external field H_{dc} was generated by a solenoid with axis perpendicular to the Earth's magnetic field to allow field variation from 0 to 70 Oe.

3. Experimental results

The variation of impedance of all samples with applied dc magnetic field has been measured by using driven ac current at $f = 310$, 510, 810, 910 and 1110 kHz, respectively. Fig. 1(a)–(c) shows three typical plots of the variation at 910 kHz for the FZBN with $x = 0$, 8 and 20 at.%, respectively (uncertainties for data in Fig. 1 are shown in Table 1). Fig. 1(a) shows that the impedance does not change with the field, indicating that no MI effect occurs in the FZBN with $x = 0$. However, as shown in Fig. 1(b), the impedance of the sample with $x = 8$ decreases with the increasing applied field, implying that the FZBN alloy with 8 at.% B displays MI effect. The large change of impedance is obtained in the sample with $x = 20$, as shown in Fig. 1(c). Similar results are obtained for the three FZBN ribbons at other frequencies.

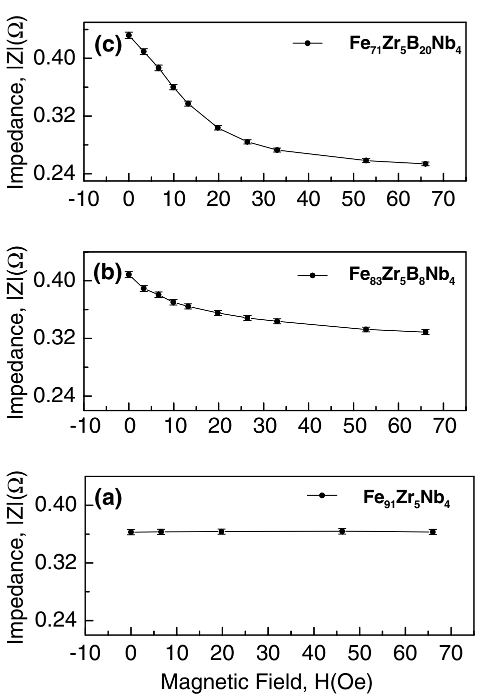

Fig. 1. Impedance as a function of external magnetic field at frequency of 910 kHz for FZBN with B content $x = 0$ (a), $x = 8$ (b) and $x = 20$ (c). Lines are provided as a guide to the eye.

The percentage change of magnetoimpedance with applied magnetic field (MI) is usually defined as [10]

$$\mathrm{MI} = \frac{\Delta Z}{Z} = \frac{Z(0) - Z(H_{sat})}{Z(H_{sat})} \times 100\%, \quad (1)$$

where $Z(0)$ and $Z(H_{sat})$ are the impedance of the sample in zero and saturation magnetic field, respectively. According to Eq. (1), we calculate MI values at various frequencies for the FZBN samples with different B contents. The changes of MI ratio with B content at various frequencies are plotted in Fig. 2 (uncertainties for data in Fig. 2 are shown in Table 3). It can be noted from Fig. 2 that MI effect is not observed for the samples with $x \leqslant 5$ but within the range of $8 \leqslant x \leqslant 30$, where the samples have been identified to be fully amorphous alloys. At frequencies below 510 kHz the MI ratio is small and changes little with B content.

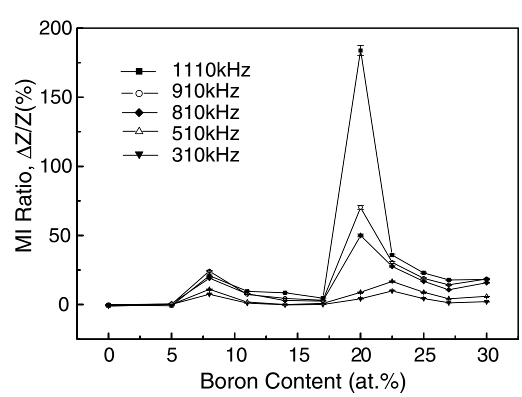

Fig. 2. Dependance of MI ratio on B content in FZBN at measuring frequency, $f = 310$, 510, 810, 910 and 1110 kHz. Lines are provided as a guide to the eye.

At higher frequencies (above 810 kHz), the value remains still small for samples within the range $5 < x \leqslant 17$, whereas for $x = 20$, the value rapidly goes up to the maximum and then, decreases slowly with the increasing B content in the range $20 < x \leqslant 30$, as shown in Fig. 2. Besides, the MI ratio at any frequency is obviously larger in high B content range ($20 < x \leqslant 30$) than in low B content range ($5 < x \leqslant 17$). More significantly, it can be seen in Fig. 2 that the sample with $x = 20$ exhibits a distinct frequency response of MI effect, while the sample with other B content does not show this character. Specially, values as large as 180% have been measured at 1110 kHz in FZBN alloys with $x = 20$, accompanied by the field sensitivity of 7%/Oe. All the fact indicates that drastic MI ratio can also be achieved for as-spun Fe-based amorphous alloys, which is completely different from the results (show very small or even no MI effect in as-spun Fe-based amorphous alloys) reported previously [1]. That large MI effect and high field sensitivity make the amorphous alloys more promising for technical applications in different kinds of high sensitivity micromagnetic sensors.

4. Discussion

Many results [3,11] indicate that the MI effect is closely related to excellent soft magnetic properties. Generally speaking, obvious MI effect can be observed in the amorphous alloys with relatively small coercive force H_c. Fig. 3 plots H_c as a function of B content for the FZBN alloys (uncertainties for data in Fig. 3 are shown in Table 1). XRD and TEM measurements have confirmed that the FZBN is crystal at $x = 0$, partial amorphous alloy at $x = 5$ and fully amorphous alloy in the range of $x = 8$–30. It is seen clearly that H_c decreases quickly in the range of $x = 5$–8, but slowly in the range of $x = 8$–30 with increasing B content, as shown in Fig. 3. That implies a strong relationship between the coercivity and the structure that small coercivity can be obtained in the fully amorphous FZBN alloys. By comparing Fig. 2 with Fig. 3, it is found that although coercive force of the samples with $x \leqslant 5$ is a few Oe larger than that of the samples with $x \geqslant 8$, the MI effect is not observed in the former composition range but in the latter, indicating that the MI effect is sensitive to the H_c. Based in Figs. 2 and 3 results, it is concluded that obvious MI effect occurs at coercivity of below 3 Oe and frequencies of above 810 kHz for the FZBN alloys. However, although the FZBN with $x = 20$ has not the smallest coercivity among all the compositions, it has distinct MI ratio at $f \geqslant 810$ kHz and approaches the maximum value of 180% at around 1.1 MHz. That indicates coercivity is not the dominant factor for the FZBN with $x = 20$ to get the drastic MI ratio, prompting us to look into the microstructures of the amorphous alloys.

It is well known that microstructure has a strong influence on both physical properties and crystallization process of melt-spun amorphous magnetic ribbons. In order to understand change of microstructure of the amorphous alloys with B content, thermal analysis was carried out carefully. Fig. 4 shows DSC curves of FZBN ($x = 8$, 14, 20, 22.5 and 30 at.%) alloys, respectively. The samples with $x < 20$ crystallizes in a primary crystallization mode, as shown in Fig. 4(a) and (b), and their crystallization products are α-Fe, $Fe_2Nb(Zr)$ and ZrB_2 [12] according to XRD results. As observed, the onset crystallization temperature changes a little with B content, while the intensity of the first exothermic peak increases with increasing B content. Both crystallization temperature and intensity of second exothermic peak of the residual amorphous alloy decrease evidently with the increment of B content. However, the increase in B content to 20 at.% causes the disappearance of the second exothermic peak of the residual amorphous alloy (see Fig. 4(c)), and the sample approximately crystallizes in an eutectic mode, without any change in crystallization products. When B content exceeds 20 at.%, as shown in Fig. 4(d) and (e), there is only one exothermic peak in the DSC curve, suggesting that the amorphous FZBN crystallizes in a eutectic mode. Moreover,

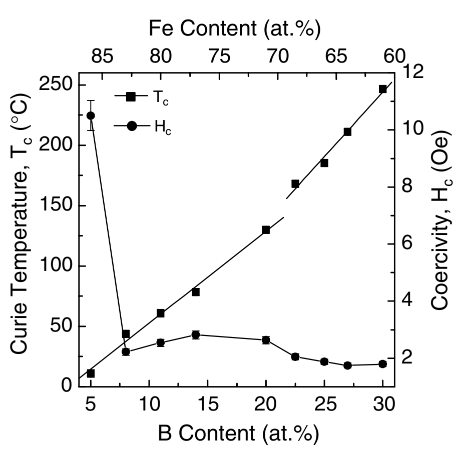

Fig. 3. Coercivity H_c and Curie temperature T_c of FZBN as a function of B content. Straight lines associated with the Curie temperature data are the result of a linear fit to these data. All other lines are provided as a guide to the eye.

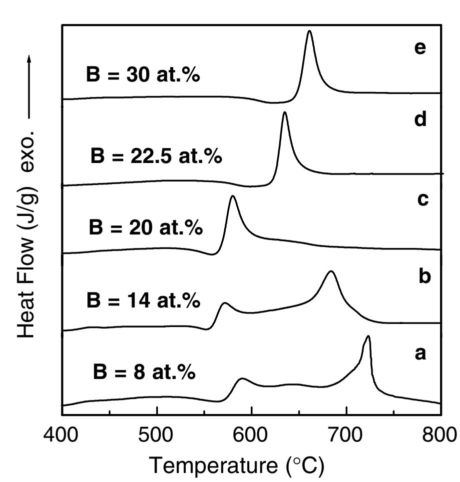

Fig. 4. DSC curves of amorphous FZBN with B content of 8 (a), 14 (b), 20 (c), 22.5 (d) and 30 (e) at.% running at 20 °C/min.

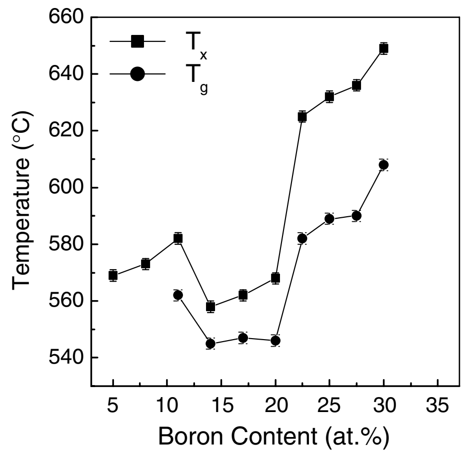

Fig. 5. Plots of crystallization temperature T_x and glass transition temperature T_g of amorphous FZBN as a function of B content. Lines are provided as a guide to the eye.

both T_x and T_g for the samples in this composition range noticeably increase all of a sudden, as observed in Fig. 5 (uncertainties for data in Fig. 5 are shown in Table 2), and also the crystallization products change into α-Fe and a new FZBN cubic phase [12]. Based on the results mentioned above, we conclude that the FZBN alloys with $x \leqslant 20$ and $x > 20$ possess different microstructures and the structure alters at the point where B content is 20 at.%.

In addition, we investigate the correlation between other physical properties and B composition. Fig. 6 shows the curves of saturated magnetization (M_s) as a function of B content at 78 K and room temperature, respectively (uncertainties for data in Fig. 6 are shown in Table 2). Both curves display evident changes at the composition of

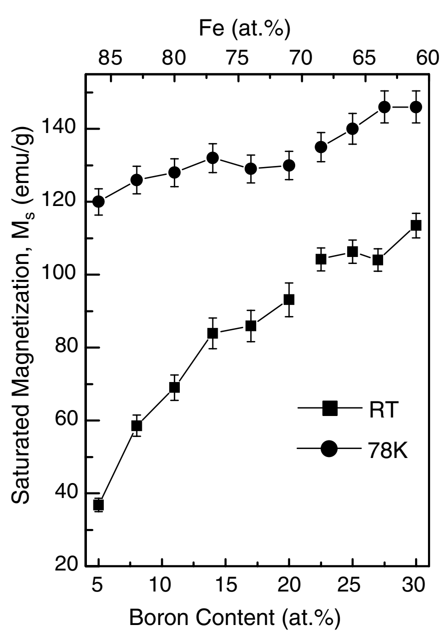

Fig. 6. Saturated magnetization as a function of B content at 78 K and room temperature for amorphous FZBN. Lines are provided as a guide to the eye.

20 at.%. According to the measurements on H_c, T_c (see Fig. 3, line is a representation of the method of linear fitting) and M_s, we can conclude that the changing tendency of these physical properties with B content in low B content range ($x \leqslant 20$) differs obviously from that in high B content range ($x > 20$) and an incontinuous change occurs at $x = 20$, which resemble the changing behavior of T_g and T_x (shown in Fig. 5). All of these consequences provide a further indication that the variation of microstructures in amorphous FZBN is responsible for its physical properties.

It is clear now that domain structures play a decisive role in the origin of the MI effect [13]. The domain wall movement contributes to the change in transverse permeability during the interaction between ac excitation field and axially applied dc magnetic field [11]. Complicated domain structure describes inhomogeneous stress distribution in different region of material. Such stress fluctuation coupled with magnetostriction produces local anisotropy which affects domain motion, and thus leads to decline in permeability and enhancement in coercive force. During the fabrication of ribbon unavoidable residual stresses remain in sample, creating irregular domain pattern. The difference of MI ratio of as-prepared samples with $0 \leqslant x \leqslant 30$ can be explained in terms of permeability changes and distinct magnetostriction constants, which have a strong relationship to their domain structures. The FZBN amorphous alloy with $x = 20$ may possess high permeability and nearly zero magnetostriction and therefore shows large MI value. However, due to the complexity of the domain structures and the domain wall motion in an applied field, as well as the lack of a good technique for characterization, its microstructure still needs to be further studied.

In conclusion, the MI effect in FZBN alloys is closely associated with the change of microstructures. The sample with B content of 20 at.% may possess special domain structure that leads to it exhibiting particular magnetic and electric properties, such as high transverse permeability. Thus, due to the fast deterioration of the permeability with the increasing applied field, skin depth rapidly increases, causing the drastic enhancement of the MI effect. Another possible mechanism responsible for the very large MI ratio in the sample with $x = 20$, may be ascribed to the small saturation magnetostriction constant resulting from its special microstructure, as many research results have proved that near zero magnetostriction can bring about significant MI effect. Anyway, the high MI ratio of the amorphous FZBN with B content of 20 at.% is not only related to coercivity but also to its special microstructure. However, the mechanism producing the distinct MI effect still needs to be studied through experiments.

5. Conclusions

The MI ratio as a function of B content has been studied for melt-spun amorphous FZBN ribbons. The MI effect, which is closely related to coercivity of the alloys, is not observed in the sample with $x \leqslant 5$, but is observed within the B-composition range between 8 and 30 at.%. A pronounced MI effect occurs at coercivities below 3 Oe and at frequencies above 810 kHz. An especially large MI effect is obtained at a saturation magnetic field of about 66 Oe in the sample with a B content of 20 at.%. As the frequency increases, the MI ratio rapidly increases, reaching a maximum value of 180% at around 1.1 MHz, with the field sensitivity of 7%/Oe. This significant MI effect is attributed to a domain structure formed by the inhomogeneous stress induced during the quenching process. As the stress varies from the surface to the center, the domain structure, as well as the magnetic anisotropy, vary along the ribbon cross-section. Due to this domain structures, the FZBN amorphous alloy with $x = 20$ may possess a high permeability and nearly zero magnetostriction. This results in the large MI effect observed.

Acknowledgements

This work is supported by the National Natural Science Foundation (grant no. 50472003), Doctoral Foundation of Education Ministry of China (grant no. 20040183063) and Creative Fund of Jilin University.

References

[1] Md. Kamruzzaman, I.Z. Rahman, M.A. Rahman, J. Mater. Process. Technol. 119 (2001) 312.
[2] K. Mohri, K. Kawashima, T. Kohzawa, H. Yoshida, L.V. Panina, IEEE Trans. Magn. 28 (1992) 3150.
[3] M. Coisson, P. Tiberto, F. Vinai, S.N. Kane, Sens. Actuators A 106 (2003) 199.
[4] R.L. Sommer, C.L. Chien, Appl. Phys. Lett. 67 (1995) 3346.
[5] S.Q. Xiao, Y.H. Liu, Y.Y. Dai, L. Zhang, S.X. Zhou, G.D. Liu, J. Appl. Phys. 85 (1999) 4127.
[6] D. Atkinson, R.S. Beach, P.T. Squire, C.L. Platt, S.N. Hogsdon, IEEE Trans. Magn. 31 (1995) 3892.
[7] M.L. Sartorelli, M. Knobel, J. Schoenmaker, J. Gutierrez, J.M. Barandiarán, Appl. Phys. Lett. 71 (1997) 2208.
[8] C. Chen, K.Z. Luan, Y.H. Liu, L.M. Mei, H.Q. Guo, B.G. Shen, J.G. Zhao, Phys. Rev. B 54 (1996) 6092.
[9] M. Tejedor, B. Hernando, M.L. Sánchez, V.M. Prida, J.M. Garcia-Beneytez, M. Vázquez, G. Herzer, J. Magn. Magn. Mater. 185 (1998) 61.
[10] F. Amalou, M.A.M. Gijs, J. Appl. Phys. 95 (2004) 1364.
[11] Md. Kamruzzaman, I.Z. Rahman, M.A. Rahman, J. Magn. Magn. Mater. 262 (2003) 162.
[12] B. Yao, Y. Zhang, L. Si, H. Tan, Y. Li, J. Alloy. Compd. 370 (2004) 1.
[13] F.L.A. Machado, C.S. Martins, S.M. Rezende, Phys. Rev. B 51 (1995) 3926.